

# Direct syntheses of $\text{La}_{n+1}\text{Ni}_n\text{O}_{3n+1}$ phases ( $n = 1, 2, 3$ and $\infty$ ) from nanosized co-crystallites

Xiaole Weng<sup>a,d</sup>, Paul Boldrin<sup>a,d</sup>, Isaac Abrahams<sup>b</sup>, Stephen J. Skinner<sup>c</sup>,  
Suela Kellici<sup>a</sup>, Jawwad A. Darr<sup>a,\*</sup>

<sup>a</sup>Department of Chemistry, Christopher Ingold Laboratories, University College London, 20 Gordon Street, London WC1H 0AJ, UK

<sup>b</sup>Centre for Materials Research, School of Biological and Chemical Sciences, Queen Mary University of London, Mile End Road, London E1 4NS, UK

<sup>c</sup>Department of Materials, Imperial College London, South Kensington, London SW7 2AZ, UK

<sup>d</sup>School of Engineering and Material Sciences, Queen Mary University of London, London E1 4NS, UK

Received 26 November 2007; received in revised form 30 January 2008; accepted 14 February 2008

Available online 10 March 2008

## Abstract

A new direct route for the “bottom up” syntheses of phases in the  $\text{La}_{n+1}\text{Ni}_n\text{O}_{3n+1}$  series ( $n = 1, 2, 3$  and  $\infty$ ) has been achieved via single-step heat treatments of nanosized co-crystallized precursors. The co-crystallized precursors were prepared using a continuous hydrothermal flow synthesis system that uses a superheated water flow at ca. 400 °C and 24.1 MPa to produce nanoparticulate slurries. Overall, a significant reduction in time and number of steps for the syntheses of  $\text{La}_3\text{Ni}_2\text{O}_7$  and  $\text{La}_4\text{Ni}_3\text{O}_{10}$  was achieved compared with more conventional synthesis methods, which typically require multiple homogenization and reheating steps over several days.

© 2008 Elsevier Inc. All rights reserved.

**Keywords:** Supercritical water;  $\text{La}_{n+1}\text{Ni}_n\text{O}_{3n+1}$  series; Solid oxide fuel cell; Continuous hydrothermal flow synthesis

## 1. Introduction

The (La–Ni–O) system forms a series of compounds with the general formula  $\text{La}_{n+1}\text{Ni}_n\text{O}_{3n+1}$ , whose structures are described by stacking along the *c*-axis of *n* finite  $\text{LaNiO}_3$  perovskite layers separated by  $\text{LaO}$  rock-salt-like layers [1] and are similar to the Ruddlesden–Popper (RP) series [2]. As a consequence of their layered framework, the RP phases can accommodate a range of non-stoichiometries and changes in the La:Ni ratio for the series can lead to very different ionic and electronic conductivity behaviors. For example, at room temperature, the  $n = 1$  and 2 compounds which correspond to the formulae  $\text{La}_2\text{NiO}_{4+\delta}$  [3–5] and  $\text{La}_3\text{Ni}_2\text{O}_{7-\delta}$  [5–7], respectively, exhibit semiconductivity, while the compounds  $\text{La}_4\text{Ni}_3\text{O}_{10-\delta}$  ( $n = 3$ ) [5,8–11] and  $\text{LaNiO}_{3-\delta}$  ( $n = \infty$ ) [12–16] were shown to be metallic. This behavior has led to them being investigated for use as cathode materials in solid oxide fuel cells

(SOFCs). Compared with traditionally used cathode materials such as  $\text{La}_{1-x}\text{Sr}_x\text{MnO}_3$  (LSM) and  $\text{La}_{1-x}\text{Sr}_x\text{Co}_{1-y}\text{Fe}_y\text{O}_3$  (LSCF), the RP phases (such as  $\text{La}_2\text{NiO}_{4+\delta}$ ) possess relatively higher oxide ion conductivity, coupled with higher mechanical and thermal stabilities at elevated operating temperatures [5]. The improved ion conductivity is caused mainly by the accommodation of hyperstoichiometric oxide ions in the rock-salt layers as interstitials in the RP structure [17]. In particular, the  $\text{La}_3\text{Ni}_2\text{O}_{7-\delta}$  and  $\text{La}_4\text{Ni}_3\text{O}_{10-\delta}$  compounds appear to possess a good balance between electronic and ionic conductivities compared with  $\text{La}_2\text{NiO}_{4+\delta}$ , which potentially make the former more promising as cathode materials in intermediate-temperature SOFCs [5,17].

The higher members of the  $\text{La}_{n+1}\text{Ni}_n\text{O}_{3n+1}$  series, particularly  $n = 2$  and 3, are difficult to synthesize in a phase pure form, normally requiring prolonged homogenization and reheating procedures [5–8,11,18]. For example, the synthesis of phase pure  $\text{La}_4\text{Ni}_3\text{O}_{10}$  typically involves heating the component metal oxide powders up to 1100 °C for 4–5 days with intermittent grinding and

\*Corresponding author. Fax: +44 207 6797463.

E-mail address: [j.a.darr@ucl.ac.uk](mailto:j.a.darr@ucl.ac.uk) (J.A. Darr).

reheating steps [8]. The large effort, high-energy costs and long time required to make these and other similarly complex binary or higher phases in a pure form, can be effectively viewed as a “bottleneck” in the discovery of new phases. Thus, there is a real need to make such complex materials more efficiently, possibly faster, in fewer steps or using less energy overall. A possible promising and direct route to the synthesis of heterometallic oxides is through heat treatment of nanoparticle co-crystallite precursors [19,20].

Continuous hydrothermal flow synthesis (CHFS) methods have offered a fast and controllable method for producing inorganic homometallic and heterometallic nanomaterials [5–8,11,18,21–29]. The basic process has been described elsewhere [30,31] and brief details will be provided herein. Recent reports have demonstrated the considerable advantages of this method in the syntheses of nanosized lithium battery materials [25,26], photocatalysts [29], bioceramics [30], ferroelectric materials [32], superconductors [19], etc. In the present work, we describe the use of nanoparticle lanthanum and nickel hydroxides co-crystallites for direct access to phases in the  $\text{La}_{n+1}\text{Ni}_n\text{O}_{3n+1}$  series ( $n = 1, 2, 3$  and  $\infty$ ).

## 2. Experimental

### 2.1. Characterizations

10 M $\Omega$  deionized (DI) water from a USF Elga water deionizer was used throughout. Ultrasonication was carried out in a VWR USC 100T ultrasonic bath at a power setting of 30 W. Gilson model 305 HPLC pumps were used in the CHFS system. Freeze drying was performed using a Vitris Advantage Freeze Dryer, Model 2.0 ES, supplied by BioPharma; the solids were frozen in liquid nitrogen and then freeze dried for 22.5 h at  $1.33 \times 10^{-4}$  MPa. In selected cases, powders were jet-milled in a Fritsch Pulverisette 7, using four 1 cm diameter stainless steel balls at a speed of 100 rpm. The constitution La/Ni atomic ratio of the products was measured using wavelength dispersion X-ray fluorescence (XRF) (ARL 9400; Ceram Research). BET surface area measurements (multipoint) were performed on a Micromeritics Gemini analyzer. All powders were degassed at 80 °C for 2 h prior to BET analysis. Particle size and morphology were investigated using a JEOL 2010 transmission electron microscope (TEM) (200 kV accelerating voltage) and a Philips XL 20 scanning electron microscope (SEM) (10–20 kV accelerating voltage). Simultaneous differential scanning calorimetry (DSC) and thermogravimetric analyses (TGA) were carried out in air using a Polymer Labs simultaneous thermogravimetric analyser (STA 1500) at a heating rate of 10 °C/min. X-ray powder diffraction (XRD) studies were conducted on a Siemens D5000 X-ray diffractometer using  $\text{CuK}\alpha$  radiation ( $\lambda = 0.15418$  nm). Data were collected over the  $2\theta$  range 5–110° with a step size of 0.02° and a count time of 10 s per step. The

diffraction patterns were analyzed by Rietveld refinement using GSAS [33]. The oxygen deficiency,  $\delta$ , was determined for heat-treated powder samples by TGA (Polymer Labs STA 1500) as follows; each sample was first heat treated in the TGA up to 300 °C in nitrogen (24 mL/min gas flow rate) at 10 °C/min and then left to dwell for 30 min at this temperature. The gas in the TGA was then switched to 5 mol%  $\text{H}_2$ -argon (24 mL/min gas flow rate) and the sample was heated from 300 to 600 °C (or up to 800 °C depending on the sample) at 2 °C/min. In experiment 8b (see Table 1), a small 5 cm, 200 W band heater (Watlow) set at 450 °C was used at the counter-current mixer (R) (see Fig. 1) [20].

## 3. General synthesis procedures

### 3.1. Materials

For all syntheses,  $\text{La}(\text{NO}_3)_3 \cdot 6\text{H}_2\text{O}$  ( $\geq 99\%$ ) and  $\text{Ni}(\text{NO}_3)_2 \cdot 6\text{H}_2\text{O}$  ( $\geq 99\%$ ) supplied by Sigma–Aldrich Chemical Company (UK), were used. Potassium hydroxide solution (KOH,  $\geq 85\%$ ) supplied by VWR International (UK) was used to adjust the pH of the metal salts.

### 3.2. Syntheses of nanosized co-crystallites in the CHFS system

The co-crystallite precursors and individual metal hydroxide slurries were manufactured using a three pump CHFS system as described elsewhere (Fig. 1) [30]. Briefly, pump P1 in Fig. 1 was used to pump water to the preheater (maintained at 400 °C), while pump P2 was used to pump the solution with a mixture of salts. Pump P3 was always used for pumping the base solution. In all cases, pump speeds were 10 mL/min, except for the superheated water (20 mL/min). This method, hereby referred to as the “hydrothermal flow coprecipitation (HFC)” method, was used to produce a range of lanthanum and nickel hydroxide co-crystallites in the desired La:Ni ratios (see Table 1). In a previous communication, we reported our initial findings for the direct syntheses of  $\text{La}_4\text{Ni}_3\text{O}_{10}$  and  $\text{La}_3\text{Ni}_2\text{O}_7$ , respectively, via a single heat treatment of the corresponding nano co-crystallites [34].

For the synthesis of the  $n = \infty$  compound ( $\text{LaNiO}_3$ ) via the HFC method, a 1:1 molar ratio of lanthanum nitrate hexahydrate and nickel nitrate hexahydrate was first prepared as follows; a 0.10 M solution of lanthanum nitrate hexahydrate and 0.10 M nickel nitrate hexahydrate in DI water were mixed together in equal volumes and stirred for 2 min. The solution was continuously pumped into the CHFS system (via a HPLC pump), whereupon it was mixed with a pumped flow of 1 M KOH solution (at point T, a  $\frac{1}{4}$  Swagelok Tee piece, Fig. 1) to give a pH of 14. Thereafter, the mixture was brought to meet the superheated water feed at 400 °C and 24.1 MPa (in a counter-current mixer as described elsewhere [31]) whereupon the hydrothermal reaction took place in a continuous fashion.

Table 1  
Details of heat treatments used for experiments 1–11, showing the products identified by XRD data

Expt.	Route	La:Ni	Heating temperature/ <sup>o</sup> C (time/h)	Product(s) identified from XRD	Particle size <sup>c</sup> (nm)	Surface area <sup>c</sup> (m <sup>2</sup> /g)	Comments
1	HFC	1:1	750(6 h)	LaNiO <sub>3</sub>	100 × 50	7.6	Phase pure material obtained
2	NPM 1	1:1	750(6 h)	La <sub>2</sub> O <sub>3</sub> <sup>a</sup> + NiO	–	–	Mixture of two separate slurries
3	NPM 2	1:1	750(6 h)	La <sub>2</sub> O <sub>3</sub> <sup>a</sup> + NiO	–	–	Dry mixed powders then dispersed <sup>b</sup>
4	HFC	4:3	450(1 h)	La <sub>2</sub> O <sub>2</sub> CO <sub>3</sub>	–	–	<sup>b</sup>
5	HFC	4:3	450(1 h) and then 750(1 h)	LaNiO <sub>3</sub> <sup>a</sup> + La <sub>2</sub> O <sub>3</sub>	–	–	<sup>b</sup>
6	HFC	4:3	450(1 h), 750(1 h) and then 1075(1 h)	La <sub>4</sub> Ni <sub>3</sub> O <sub>10</sub> <sup>a</sup> + La <sub>2</sub> O <sub>2</sub> CO <sub>3</sub>	–	–	Includes a jet-milling step <sup>b</sup>
7	HFC	4:3	1075(1 h)	La <sub>4</sub> Ni <sub>3</sub> O <sub>10</sub> <sup>a</sup> + La <sub>2</sub> NiO <sub>4</sub>	–	–	<sup>b</sup>
8a	HFC	4:3	1075(12 h)	La <sub>4</sub> Ni <sub>3</sub> O <sub>10</sub>	249 ± 41	2.1	Phase pure material obtained <sup>d</sup>
8b	HFC	4:3	1075(6 h)	La <sub>4</sub> Ni <sub>3</sub> O <sub>10</sub>	–	–	Phase pure material obtained <sup>d</sup> Water was heated to 450 °C and an additional band heater (450 °C) was used <sup>b</sup>
9	HFC	3:2	1150(7 h)	La <sub>3</sub> Ni <sub>2</sub> O <sub>7</sub> <sup>a</sup> + La <sub>2</sub> NiO <sub>4</sub>	–	–	<sup>b</sup>
10	HFC	3:2	1150(12 h)	La <sub>3</sub> Ni <sub>2</sub> O <sub>7</sub>	424 ± 80	<1	Phase pure material obtained <sup>d</sup>
11	HFC	2:1	1000(6 h)	La <sub>2</sub> NiO <sub>4</sub>	127 ± 20	4.1	Phase pure material obtained

Note: when more than one heat treatment was applied, the powder was cooled down to room temperature (RT) before the next heat treatment.

<sup>a</sup>Major phase as observed in the XRD data.

<sup>b</sup>No NiO was observed in the XRD pattern but its presence is inferred from the reagent stoichiometry and other lanthanum-containing phases identified.

<sup>c</sup>Data are for heat-treated samples.

<sup>d</sup>Conventional synthesis = several days heat treatment and regrind [5–8,11,12,18].

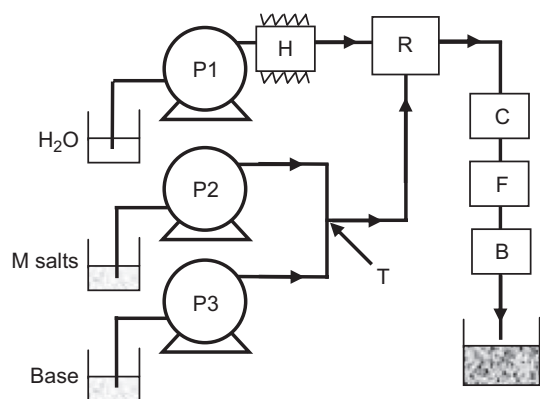


Fig. 1. Scheme of the three-pump continuous hydrothermal flow synthesis system used for the syntheses of nanoparticles. Key: P = pump, C = cooling, F = filter, B = backpressure regulator, R = reactor, T = stainless steel “Tee” piece mixer and H = heater.

The slurry from the CHFS system was collected at the exit of the back-pressure regulator (at ambient pressure) for approximately 50 ml in 50 mL falcon tubes (pH at this point was 14). Each filled falcon tube was centrifuged (4500 rpm for 3 min). 40 mL of clear liquid was removed and then replaced with 40 mL of clean DI water with shaking to disperse the solids. Each falcon tube was further centrifuged (4500 rpm for 3 min) and the clear liquid was removed again. The resulting wet solids were freeze dried. According to the dried mass, the yield was calculated as 87%. Heat treatment was carried out in a furnace in air

according to the conditions as described in Table 1 (experiment 1).

To produce the co-crystallized precursor for the  $n = 3$  compound (La<sub>4</sub>Ni<sub>3</sub>O<sub>10</sub>) (experiments 4–8), a solution with a 4:3 molar ratio of La:Ni nitrates was prepared (0.10 and 0.075 M with respect to La and Ni containing solutions). Thereafter, an identical method to that described earlier was employed. The yield for this reaction was calculated as 85% based on dry mass. Table 1 details the subsequent heat treatment of this powder (experiments 4–8). Similarly, for the  $n = 2$  (La<sub>3</sub>Ni<sub>2</sub>O<sub>7</sub>) and  $n = 1$  (La<sub>2</sub>NiO<sub>4</sub>) compounds, 3:2 and 2:1 molar ratios of La:Ni nitrates, respectively, were prepared (0.12:0.08 M and 0.1:0.05 M with respect to La:Ni, respectively). The yields based on dried masses were calculated as 87% and 91% for the 3:2 and 2:1 compounds, respectively, based on dry mass. Again, Table 1 details the heat treatment regimes used for both the 3:2 La:Ni ratio (experiments 9 and 10) and the 2:1 La:Ni ratio powders (experiment 11).

As a set of control experiments, separate slurries of nanosized lanthanum hydroxide and nickel hydroxide were manufactured by the CHFS method and then attempts were made to homogenize these powders (nanoparticle mixing methods, NPMs). Brief experimental details are given below.

### 3.3. Syntheses of individual nanoparticle slurries and dried powders for use in NPM experiments

Separate lanthanum and nickel hydroxide slurries were manufactured in the CHFS system using 0.10 M metal salt

solutions. In each case, the respective metal salt solution was pumped to meet a 1 M KOH solution at point T to give a pH of 14 in the CHFS system. The mixtures then came into contact with the superheated water flow in a similar manner to that described earlier. Each slurry was also initially cleaned up in an identical manner to that described earlier for the HFC route. The cleaned  $\text{La}(\text{OH})_3$  slurry was found to contain 3.49 wt% solids in water, while the cleaned  $\text{Ni}(\text{OH})_2$  slurry contained 1.84 wt% solids in water (supplementary data S1). Yields were calculated as 89% and 91%, for  $\text{La}(\text{OH})_3$  and  $\text{Ni}(\text{OH})_2$ , respectively, based on dry masses. Having produced the individual metal hydroxide slurries, two methods for producing homogenized materials were attempted, namely NPM1 and NPM2. Details are given below.

### 3.3.1. Nanoparticle mixing type 1 (NPM1)

The individual  $\text{La}(\text{OH})_3$  and  $\text{Ni}(\text{OH})_2$  slurries were mixed in a 1:1 molar ratio as follows; 20 mL of the stirred lanthanum hydroxide slurry (0.022 M) and 29 mL of the nickel hydroxide slurry (0.153 M) were accurately measured into a beaker using a syringe and stirred. The resulting slurry was ultrasonicated for 20 min at 30 W and was then centrifuged at 4500 rpm for 3 min with 40 mL of liquid removed. The wet solids were freeze dried and then heat treated in a furnace in air according to the time and temperature as described in Table 1. This route is referred to as NPM1 (experiment 2).

### 3.3.2. Nanoparticle mixing type 2 (NPM2)

As an alternative route to NPM1, each of the metal hydroxide slurries was first freeze dried and the powders were dry mixed as follows; for a 1:1 molar ratio of La:Ni, freeze-dried lanthanum hydroxide nanopowder (0.4832 g, 0.025 mol) and nickel hydroxide (0.2606 g, 0.025 mol) nanopowder were accurately weighed, hand mixed briefly and added to DI water (25 mL) in a beaker. The slurry was ultrasonicated for 20 m at 30 W, was centrifuged at 4500 rpm for 3 min and 20 mL of liquid was removed (Supplementary data S2). The wet solids were freeze dried and the powder was then heat treated in a furnace in air according to the time and temperature described in Table 1. This method is referred to as nanoparticle mixing type 2, i.e. NPM2 (experiment 3).

## 4. Results and discussion

### 4.1. Syntheses of target compounds

The individual nanoparticle metal hydroxide precursors used for the two NPM routes were characterized by XRD and were found to be nickel hydroxide (good match to JCPDS pattern 14-011, Supplementary Fig. S1a) and lanthanum hydroxide (good match to JCPDS pattern 36-1481, Supplementary Fig. S1b), respectively, as expected. TEM images revealed that the nickel hydroxide consisted of hexagon-like plates ca. 80 nm in diameter (Fig. 2a). The

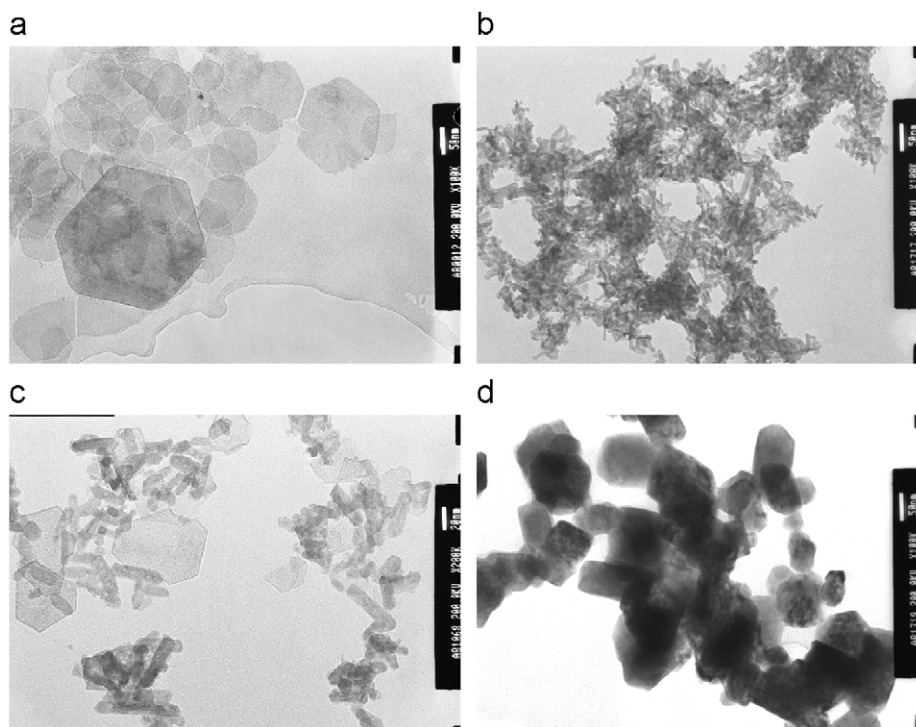


Fig. 2. Transmission electron microscope images of (a) nickel hydroxide nanoparticles (bar = 50 nm), (b) lanthanum hydroxide nanoparticles (bar = 50 nm), (c) as-prepared metal hydroxide co-crystallized powder with a 4:3 molar ratio of La:Ni (bar = 20 nm) made in the continuous hydrothermal flow synthesis system, using a superheated water feed at 400 °C and 22.1 MPa and (d) phase pure  $\text{LaNiO}_3$  made by a single heat treatment at 750 °C for 6 h in air (bar = 50 nm).

lanthanum hydroxide particles were found to exist as ca. 40 nm × 10 nm needles (Fig. 2b). The XRD data for the nano co-crystallite powder with a 4:3 La:Ni molar ratio of the metal hydroxides (made in the CHFS system via the HFC route), suggested a mixture of lanthanum hydroxide and nickel hydroxide was present as expected (Supplementary Fig. S1c). TEM analysis of the nanopowder (with 4:3 La:Ni ratio) showed intimately mixed crystalline nickel hydroxide and lanthanum hydroxide particles, which were similar in size and shape to those observed in the individual slurries (respective compounds were confirmed by energy dispersive X-ray spectroscopy) (Fig. 2c). The specific BET surface areas for the co-crystallites (with 4:3 La:Ni ratio), individual lanthanum hydroxide and nickel hydroxide powders were measured at 82, 104 and 135 m<sup>2</sup>/g, respectively.

Synthesis of the target compound of LaNiO<sub>3</sub> was attempted via three different routes; a “HFC” route and two NPM” routes (experiments 1–3, respectively). For the HFC route (experiment 1), a co-crystallized mixture of lanthanum and nickel hydroxides in a 1:1 molar ratio was made inside the CHFS system. For the NPM routes, the individual lanthanum and nickel hydroxide slurries were separately prepared and then mixed in a 1:1 molar ratio without any initial drying prior to mixing (NPM1 route) and with a drying step prior to physical mixing (NPM2). We were interested to discover how these different mixing approaches would affect the products obtained upon heat treatment. Table 1 shows the various routes and heat treatments that were employed.

The heat treatment conditions used for the 1:1 molar ratio mixtures were suggested from the previous reports in the literature, [16,35–38] where a mixture of La(NO<sub>3</sub>)<sub>3</sub> and Ni(NO<sub>3</sub>)<sub>2</sub>, diluted in aqueous KOH or organic compounds, gave the pure LaNiO<sub>3</sub> phase after 4–8 h heat treatment at ca. 750 °C. In our work, the XRD data of the product from heat treatment of the HFC co-crystallite at 750 °C for 6 h in air (experiment 1), showed a good match with LaNiO<sub>3</sub> (JCPDS pattern 34-1028, Fig. 3). TEM images of LaNiO<sub>3</sub>

from experiment 1, revealed that the 6 h heat-treated product had formed rhombohedral agglomerates of ca. 50 nm × 100 nm primary particle size (Fig. 2d). The corresponding specific BET surface area was 7.6 m<sup>2</sup>/g.

In contrast to the aforementioned HFC route, an identical heat treatment (750 °C/6 h) was performed on the 1:1 La:Ni molar ratio metal hydroxide mixtures prepared via the NPM1 and NPM2 routes (experiments 2 and 3, respectively). Surprisingly, the XRD data of the heat-treated products suggested that only a mixture of La<sub>2</sub>O<sub>3</sub> and NiO had been obtained in both cases (Supplementary Fig. S2a and S2b for NPM 1 and 2 routes, respectively). Even after the product from experiment 2 was jet-milled at 100 rpm for 1 h, and then heat treated for a second time (750 °C for 10 h), there was no suggestion of any LaNiO<sub>3</sub> formation in our experiment (Supplementary Fig. S2c). This implies that the metal hydroxides were not sufficiently homogenized through the NPM routes, even after additional milling. In contrast, the HFC route (experiment 1) yielded intimately mixed precursors (i.e. a co-crystallite), leading to fast and efficient syntheses of the corresponding heterometallic compounds. Compared with more conventional room temperature batch coprecipitation syntheses, where several phases can be formed at different times during the precipitation process, the CHFS method ensures both phases are rapidly and simultaneously formed and are intimately mixed. This allows us to overcome limitations of insufficient mass transfer that would normally exist for less well homogenized nanoparticle mixtures.

It is widely reported that the higher order RP phases such as La<sub>4</sub>Ni<sub>3</sub>O<sub>10</sub>, in particular, are difficult to prepare and normally require heating at or above 1000 °C and rehomogenization steps over several days [8,11,18,39]. We postulated that the high intimacy of mixing afforded for the metal hydroxides in the co-crystallites from the HFC route, may be advantageous to the efficient synthesis of La<sub>4</sub>Ni<sub>3</sub>O<sub>10</sub>. Initially, STA of a 4:3 molar ratio La:Ni metal hydroxide co-crystallite was carried out over the temperature range 20–1100 °C (in air), to suggest likely temperatures at which phase transformations might occur, albeit under non-equilibrium conditions (Supplementary Fig. S3). The STA data suggested at least six overlapping regions of weight loss between 20 and 1100 °C, these were in the ranges 20–174 °C (9.22% weight loss), 174–270 °C (2.71% weight loss), 270–377 °C (4.66% weight loss), 377–487 °C (1.21% weight loss), 487–789 °C (1.58% weight loss) and 789–1100 °C (decomposition and ongoing weight loss). In the temperature range 20–487 °C, endothermic peaks were centered at 87 °C (weak, broad), 223 °C (weak, broad), 320 °C (strong, sharp) and 426 °C (weak, sharp), respectively. Presumably, these corresponded to the loss of adsorbed water, dehydration of Ni(OH)<sub>2</sub>, partial dehydration of La(OH)<sub>3</sub> and possibly some dehydration of LaOOH, respectively. Thereafter, between ca. 487 and 789 °C (a weak and broad exothermic peak was centered at 580 °C in this region), it is assumed the reaction of La<sub>2</sub>O<sub>3</sub>

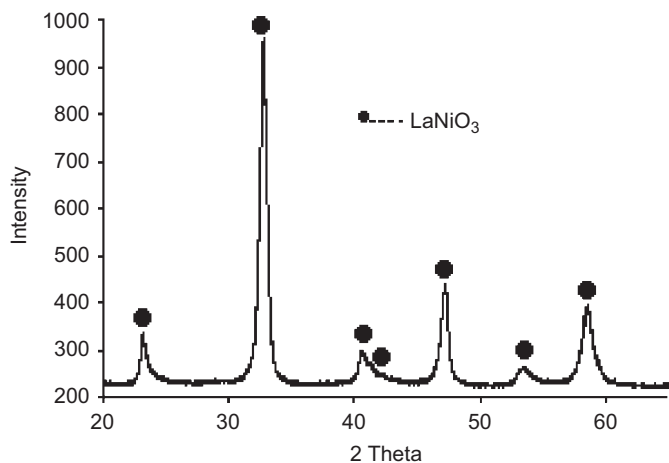


Fig. 3. X-ray diffraction pattern of the products from heat treatment (750 °C for 6 h in air) of the metal hydroxide co-crystallized mixture with a 1:1 La:Ni ratio.

(or a similar species) and NiO took place to form  $\text{LaNiO}_3$  (uptaking some oxygen in this reaction). The small weight loss that was observed in this range is presumable due to completion of the dehydration of the La-hydroxy containing species upon conversion to  $\text{LaNiO}_3$  and some oxygen loss after conversion to  $\text{LaNiO}_3$ . Finally, above  $789^\circ\text{C}$ , the decomposition of  $\text{LaNiO}_3$  was observed, presumably forming  $\text{La}_4\text{Ni}_3\text{O}_{10}$  or other RP phases. The supplementary section (Supplementary Fig. S3a and S3b, respectively) contains the TGA and DSC data for the 4:3 ratio nanopowder, the pure  $\text{La}(\text{OH})_3$  powder and the  $\text{Ni}(\text{OH})_2$  nanopowder, respectively. As can be seen from these figures, the DSC and TGA plots for the 4:3 nanopowder co-crystallites do not show great similarities to the respective metal hydroxides, thus actual weight loss assignments for the former are in fact quite difficult. It should be noted that the overall weight loss (based on dry mass) between  $174^\circ\text{C}$  (when all weakly bound water is removed to leave  $\text{La}(\text{OH})_3$  and  $\text{Ni}(\text{OH})_2$ ) and  $789^\circ\text{C}$  (when  $\text{LaNiO}_3$  is presumed to have been formed) was ca. 11.19 wt%. The STA data were used for the selection of heating temperatures (see below) in a set of further experiments (experiments 4–8).

A dried co-crystalline mixture made in the CHFS system with a 4:3 molar ratio of La:Ni salts in the solution feed was heat treated at  $450^\circ\text{C}$  for 1 h (experiment 4; HFC route). The XRD pattern of the product showed a good match with  $\text{La}_2\text{O}_2\text{CO}_3$  (JCPDS 22–1127, Supplementary Fig. S4a). No Ni containing species were observed in the XRD data. TEM images of the product (Supplementary Fig. S5) suggested that  $\text{La}_2\text{O}_2\text{CO}_3$  particles surround NiO particles, and possibly shield them. Interestingly, it was reported that carbonation of  $\text{La}_2\text{O}_3$  to form  $\text{La}_2\text{O}_2\text{CO}_3$  can be catalyzed by the presence of NiO [40–42], which could explain why  $\text{La}_2\text{O}_2\text{CO}_3$  was produced rather than  $\text{La}_2\text{O}_3$ . We also conducted an identical experiment with degassing of all solutions which gave the same products, thus, as expected, carbonate is formed as a result of  $\text{CO}_2$  being adsorbed from the air during heat treatment and that NiO acts as a catalyst for its formation. This was further evidenced by heat treatment of the co-crystallized mixture (La/Ni ratio at 4:3) at  $450^\circ\text{C}$  for 1 h in argon in a tube furnace, which according to the XRD data revealed broad peaks which were due to a mixture of  $\text{La}_2\text{O}_3$  (JCPDS 00–004–0856) and NiO (JCPDS 00–004–0835) and no lanthanum carbonate (see Supplementary Fig. S4d).

The heat-treated sample from experiment 4 was subsequently subjected to a further heat treatment in a furnace at  $750^\circ\text{C}$  for 1 h in air (experiment 5), yielding  $\text{LaNiO}_3$  as a major phase (JCPDS 34–1028) and  $\text{La}_2\text{O}_3$  as a minor phase (good match to JCPDS 05–0602) (Supplementary Fig. S4b). This is unsurprising given the initial 4:3 mol ratio of La:Ni. In this case, presumably decomposition of  $\text{La}_2\text{O}_2\text{CO}_3$  to lanthanum oxide and  $\text{CO}_2$  [43] occurred prior to the formation of  $\text{LaNiO}_3$ . The reason for the observation of  $\text{La}_2\text{O}_3$  rather than  $\text{La}_2\text{O}_2\text{CO}_3$  was assumed to be due to a deficiency of NiO catalyst, as it had been consumed to make  $\text{LaNiO}_3$ . The product from experiment 5 was

subjected to yet another heat treatment at  $1075^\circ\text{C}$  for 1 h (experiment 6). This heating temperature is similar to that reported in the literature for the production of  $\text{La}_4\text{Ni}_3\text{O}_{10}$  [11]. This experiment yielded a mixture of  $\text{La}_4\text{Ni}_3\text{O}_{10}$  (JCPDS 35–1242) and  $\text{La}_2\text{O}_2\text{CO}_3$  (JCPDS 23–322) (Supplementary Fig. S4c). In this case, the formation of  $\text{La}_2\text{O}_2\text{CO}_3$  may have been favored by the presence of excess NiO released through the decomposition of  $\text{LaNiO}_3$  (Eq. (1)) [44]. Further heat treatments of this product only seemed to increase the crystallinity of the impurity, indicating that irreversible phase segregation had taken place through multiple heat treatment steps (for details see Supplementary data S3):



With the aforementioned results in mind, a 4:3 molar ratio La:Ni co-crystallite powder was directly heated to  $1075^\circ\text{C}$  for 1 h (Fig. 4a(i)) (HFC method; experiment 7). XRD analysis revealed that the products were a mixture of

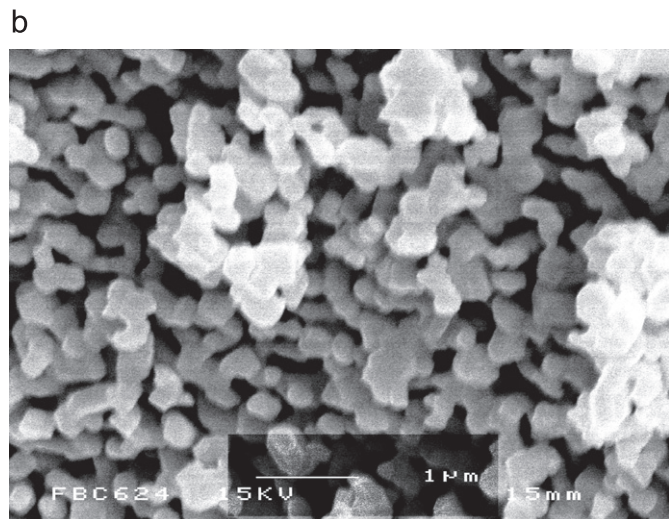
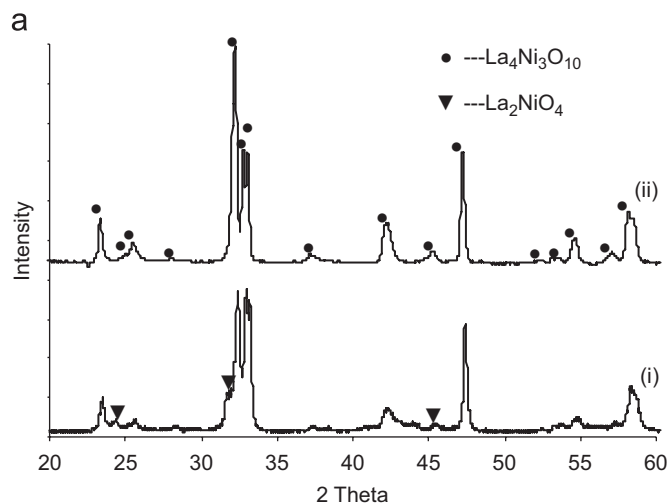


Fig. 4. (a) X-ray diffraction patterns of the products made by heat treatment ( $1075^\circ\text{C}$  in air) of metal hydroxide co-crystallized powders with a 4:3 La:Ni molar ratio, for (i) 1 h and (ii) 12 h and (b) scanning electron microscope image of  $\text{La}_4\text{Ni}_3\text{O}_{10}$  made by a single heat treatment at  $1075^\circ\text{C}$  for 12 h in air (bar =  $1\ \mu\text{m}$ ).

$\text{La}_4\text{Ni}_3\text{O}_{10}$  and  $\text{La}_2\text{NiO}_4$  (instead of  $\text{La}_2\text{O}_2\text{CO}_3$ ). Again, NiO was not observed in the diffraction patterns. After further investigation, it was found that phase pure  $\text{La}_4\text{Ni}_3\text{O}_{10}$  compound could be obtained directly from a HFC co-crystallite with a 4:3 ratio after at least 12 h heat treatment at 1075 °C [Fig. 4a(ii)] (experiment 8a). This was a significant result, as to our knowledge, this material has not directly been made from any similar mixture in a single heat treatment step [34]. We suggest that the successful single-step synthesis of  $\text{La}_4\text{Ni}_3\text{O}_{10}$  (not requiring any regrinding steps), was due to the high intimacy of mixing in the co-crystallites (made in the CHFS system), which facilitated efficient mass transfer during the minimum of 12 h heat treatment (conventional synthesis requires up to 14 days [7]). After the success of this reaction, we subsequently tried to make the 4:3 co-crystallite using rather more severe conditions, in which  $\text{H}_2\text{O}_2$  was added in metal solution (pump 2), a band heater (set to 450 °C) was placed on the outside of the counter-current reactor and the superheated water was set to 450 °C (rather than 400 °C). This time the “co-crystallized” powder obtained was believed to be a mixture of  $\text{La}(\text{OH})_3$  and NiO (rather than  $\text{Ni}(\text{OH})_2$  as previously reported [20]), although the XRD data did not reveal any NiO characteristic peaks (see Supplementary Fig. 6a). This presumption for NiO has been made on the basis of recently published research by our group [20] that shows NiO can be produced at 450 °C (inlet water temperature) with peroxide added and an external band heater at the mixing point set to 450 °C. Interestingly, a single heat treatment of this as-prepared powder at 1075 °C for 6 h was sufficient to obtain phase pure  $\text{La}_4\text{Ni}_3\text{O}_{10}$  (this is experiment 8b, see Supplementary Fig. 6b), which is a 50% further decrease in synthesis time [34]. This result suggested that the synthesis parameters such as presence of  $\text{H}_2\text{O}_2$ , the increase of superheated water temperature, adding a band heater and other factors can lead to a more facile synthesis during subsequent heat treatment of the “as-crystallized” nanopowder.

Overall, our experimental observations appear to be consistent with the thermodynamic study of the La–Ni–O system by Zinkevich and Aldinger [45,62], who indicated that the formation of an intermediate phase,  $\text{La}_2\text{NiO}_4$ , was itself made by the reaction of  $\text{La}_2\text{O}_3 + \text{NiO}$  above 1000 °C (Eq. (2)):



The relative thermodynamic stabilities of the lanthanum nickelate phases are reported to be in the order  $\text{La}_2\text{NiO}_4 > \text{La}_3\text{Ni}_2\text{O}_7 > \text{La}_4\text{Ni}_3\text{O}_{10} > \text{LaNiO}_3$ , with the decomposition of  $\text{LaNiO}_3$  (Eq. (3)) estimated at around  $980 \pm 20$  °C [45].



As indicated in several published works,  $\text{La}_4\text{Ni}_3\text{O}_{10}$  would be expected to be thermodynamically accessible via the reaction of  $\text{La}_3\text{Ni}_2\text{O}_7$  and NiO at ca. 1075 °C. However, experimental data in the literature reveal that  $\text{La}_4\text{Ni}_3\text{O}_{10}$  is

in fact formed via the direct reaction of in-situ formed  $\text{La}_2\text{NiO}_4$  and NiO in air (Eq. (4)) [45,46]. The inability to make  $\text{La}_4\text{Ni}_3\text{O}_{10}$  via a  $\text{La}_3\text{Ni}_2\text{O}_7$  phase under such conditions is largely because in-situ solid state formation of the latter phase is very slow (assuming the homometallic oxides are used as the starting materials) and therefore, the faster route involving in-situ formation of  $\text{La}_2\text{NiO}_4$  is observed. It is however clear that the thermodynamic stabilities as a function of both temperature and oxygen partial pressure are complex in this system with the exact decomposition mechanisms the subject of some speculation, particularly regarding the  $\text{La}_4\text{Ni}_3\text{O}_{10}$  and  $\text{LaNiO}_3$  phases [62,63].

SEM analysis of the phase pure  $\text{La}_4\text{Ni}_3\text{O}_{10}$ , revealed rounded agglomerated particles with a primary particle size of  $249 \pm 41$  nm (range 153–336 nm based on 50 particles, Fig. 4b). To the best of our knowledge, synthesis methods for successfully producing submicron  $\text{La}_4\text{Ni}_3\text{O}_{10}$  particles have not been reported before. The corresponding specific surface area characterized by BET was measured at  $2.1 \text{ m}^2/\text{g}$ :



Similarly to  $\text{La}_4\text{Ni}_3\text{O}_{10}$  ( $n = 3$ ),  $\text{La}_3\text{Ni}_2\text{O}_7$  ( $n = 2$ ) is known to be difficult to synthesize directly, typically involving several days of intermittent regrinding and reheating steps [5–7,11,18]. Further experiments (using the HFC route), involving a 3:2 molar ratio La:Ni co-crystallite, were conducted in an attempt to synthesize  $\text{La}_3\text{Ni}_2\text{O}_7$ . Simultaneous thermal analysis data (TGA/DSC) for the corresponding co-crystallite prior to heat treatment suggested that the phase transition temperature for  $\text{La}_3\text{Ni}_2\text{O}_7$  may occur in the region 1000–1150 °C (Supplementary Fig. S7a), which is in agreement with the literature (ca. 1150 °C) [6]. Using the HFC route, the corresponding co-crystallite mixture (with a 3:2 molar ratio of La:Ni) was heat treated at 1150 °C in air for 7 h (experiment 9). The XRD data of the heat-treated product revealed peaks due to both  $\text{La}_3\text{Ni}_2\text{O}_7$  (major phase) and  $\text{La}_2\text{NiO}_4$  (JCPDS pattern 34-0314) (Fig. 5a(i)), which indicated incomplete conversion to the target in the allotted time. When a virtually identical heat treatment was instead conducted for a longer time of 12 h (experiment 10), phase pure  $\text{La}_3\text{Ni}_2\text{O}_7$  (JCPDS pattern 35-1243) was obtained (Fig. 5a(ii)). SEM analysis of the phase pure  $\text{La}_3\text{Ni}_2\text{O}_7$  product from experiment 10 revealed rounded agglomerated particles with a primary particle size of  $424 \pm 80$  nm (range 335–625 nm based on 50 particles; Fig. 5b). Similar to the case of  $\text{La}_4\text{Ni}_3\text{O}_{10}$ , to our knowledge, there has been no previous report on the direct synthesis of submicron  $\text{La}_3\text{Ni}_2\text{O}_7$  particles. The corresponding specific surface area of  $\text{La}_3\text{Ni}_2\text{O}_7$  powder characterized by BET was measured at less than  $1 \text{ m}^2/\text{g}$ .

NPM experiments for 4:3 and 3:2 La:Ni ratios were also carried out. These were unsuccessful in achieving the respective targets in pure form, and resulted in the formation of a mixture of  $\text{La}_2\text{NiO}_4$  and  $\text{La}_2\text{O}_3$  in both cases [34].

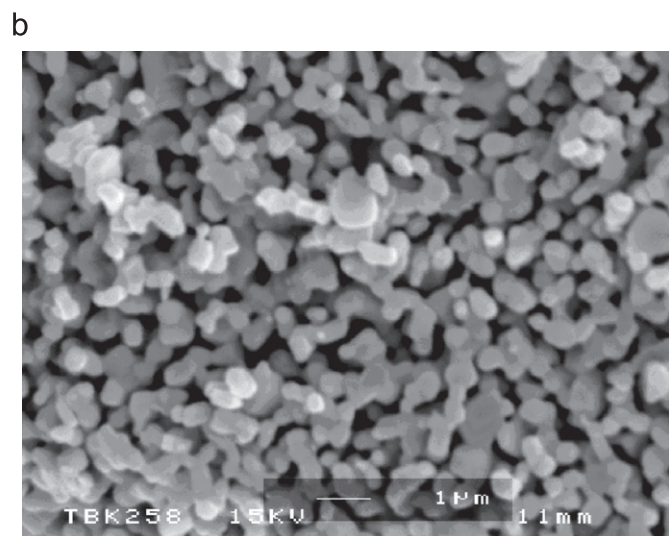
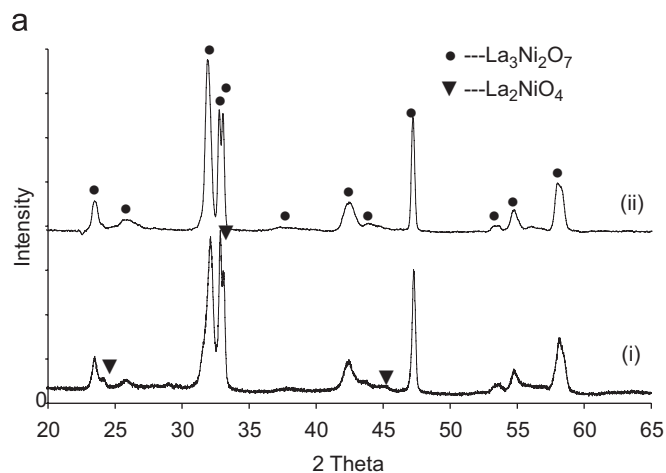


Fig. 5. (a) X-ray diffraction patterns of the products made by heat treatment (1150 °C in air) of a nanoparticle metal hydroxide co-crystallized mixture with a 3:2 La:Ni molar ratio, for (i) 7 h and (ii) 12 h and (b) Scanning electron microscope image of  $\text{La}_3\text{Ni}_2\text{O}_7$  made by a single heat treatment at 1150 °C for 12 h in air (bar = 1  $\mu\text{m}$ ).

Finally, a co-crystallized powder with a 2:1 molar ratio of La:Ni was prepared in an attempt to synthesize  $\text{La}_2\text{NiO}_4$  (HFC route). Initially, the STA data for this 2:1 co-crystallite (prior to heat treatment) suggested that a phase transition temperature for  $\text{La}_2\text{NiO}_4$  may exist in the range 1000–1100 °C (Supplementary Fig. S7b). The critical conditions for the syntheses of pure  $\text{La}_2\text{NiO}_4$  or other related compounds are known to be determined by several factors; the heating temperature and time, the oxygen partial pressure, the homogeneity of the starting materials and the initial particle size [6]. Synthesis of  $\text{La}_2\text{NiO}_4$  has been previously reported over a wide temperature range 850–1400 °C in the literature [4,5,47–50]. Consequently, phase pure  $\text{La}_2\text{NiO}_4$  (JCPDS pattern 34-0314) was obtained in this work by heat treatment of the corresponding co-crystallite at 1000 °C for 6 h (Fig. 6a). SEM analysis revealed rounded agglomerated particles with a primary particle size of  $127 \pm 20$  nm (range 75–163 nm based on 50

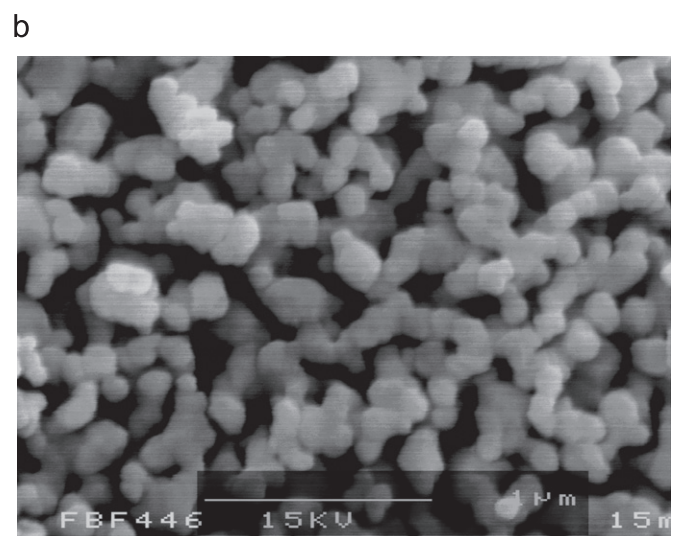
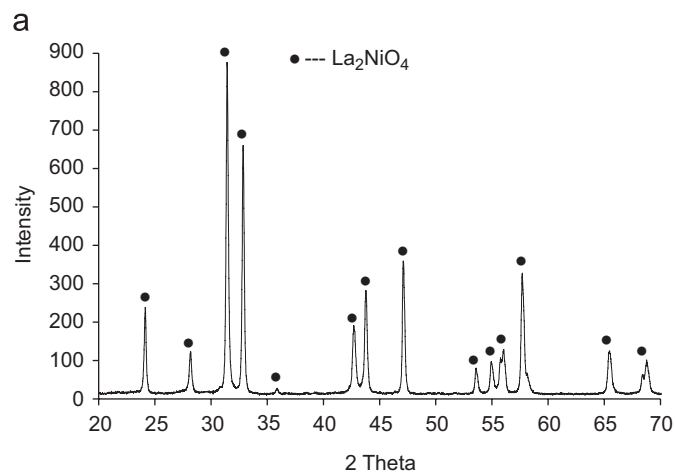


Fig. 6. (a) X-ray diffraction pattern of the products made by heat treatment (1000 °C for 6 h in air) of a nanoparticle metal hydroxide co-crystallized mixture with a 2:1 La:Ni ratio) and (b) scanning electron microscope image of  $\text{La}_2\text{NiO}_4$  by a single heat treatment at 1000 °C for 6 h (bar = 1  $\mu\text{m}$ ).

particles; Fig. 6b). The corresponding specific BET surface area of the  $\text{La}_2\text{NiO}_4$  powder was 4.1 m<sup>2</sup>/g.

#### 4.2. Structural and constitutional characterization

The XRD patterns for the La–Ni–O compounds were analyzed by Rietveld refinement. Application of the previously reported rhombohedral structure [51] and tetragonal structure [52] as starting models lead to the identification of  $\text{LaNiO}_3$  phase as being  $R\bar{3}c$  ( $R_{\text{wp}} = 0.0965$ ,  $R_{\text{p}} = 0.0730$ ) and  $\text{La}_2\text{NiO}_4$  phase as  $I4/mmm$  ( $R_{\text{wp}} = 0.1283$ ,  $R_{\text{p}} = 0.0972$ ). The previously reported face centered structures [6,8] were used as starting models for refinement of the  $n=2$  and 3 compounds and gave satisfactory fits to  $\text{La}_3\text{Ni}_2\text{O}_7$  ( $R_{\text{wp}} = 0.1277$ ,  $R_{\text{p}} = 0.0944$ ) and  $\text{La}_4\text{Ni}_3\text{O}_{10}$  ( $R_{\text{wp}} = 0.1234$ ,  $R_{\text{p}} = 0.0868$ ) in space group  $Fm\bar{3}m$ . It is noted here that neutron diffraction patterns of these two phases are more accurately described in space

Table 2

Refined unit-cell parameters (nm, by XRD), oxygen deficiency (–) (or hyperstoichiometry (+)) parameter ( $\delta$ , by TGA) and the constitution atomic ratio for lanthanum nickel oxides

$n$	$a$ (nm)	$b$ (nm)	$c$ (nm)	Space group	La:Ni	$\delta$
$\infty$	0.54515(5)	0.54515(5)	1.3168(2)	$R\bar{3}c$	0.96:1	$-0.09(2)$
1	0.386207(9)	0.386207(9)	1.26977(4)	$I4/mmm$	1.94:1	$+0.18(3)$
2	0.54204(9)	0.54620(9)	2.0455(4)	$Fmmm$	2.92:2	$+0.08(5)$
3	0.54126(6)	0.54595(6)	2.8021(4)	$Fmmm$	3.90:3	$-0.46(6)$

Estimated standard deviations are given in parentheses.

groups  $Bmab$  and  $Amam$ , respectively [7]. However, refinement in these lower symmetry space groups failed to converge. The refined unit-cell parameters are summarized in Table 2.

The constitution atomic ratios of the products were characterized using XRF, yielding the La/Ni ratio in  $\text{La}_3\text{Ni}_2\text{O}_7$  at 1.46 (expected value 1.50),  $\text{La}_4\text{Ni}_3\text{O}_{10}$  at 1.30 (expected value 1.33),  $\text{LaNiO}_3$  at 0.96 (expected value 1) and  $\text{La}_2\text{NiO}_4$  at 1.94 (expected value 2). The very slight deficiency in La is due to the relatively lower yield of  $\text{La}(\text{OH})_3$  precursor during the co-precipitation. These measured values were used along with the thermogravimetric analytical data (see below) to calculate the oxygen hyperstoichiometry/deficiency parameters,  $\delta$ , for each of the products.

In order to calculate the oxygen deficiency (or hyperstoichiometry) parameter,  $\delta$ , for phase pure La–Ni–O compounds, simultaneous TGA were performed under a flowing 5%  $\text{H}_2$ –argon gas mixture by heating samples at 2 °C/min from room temperature to 600 °C (for  $n = \infty$  compound), 700 °C (for  $n = 2$  and 3 compounds), and 800 °C (for  $n = 1$  compound). The delta values were calculated by assuming that the respective La–Ni–O compounds were reduced in the TGA apparatus to a mixture of lanthanum(III) oxide and metallic nickel after heating to the target temperatures (Supplementary Fig. S4e for the XRD data, which supports this assumption). TGA plots are contained in the Supplementary data (Fig. S8), while full calculations are given in Supplementary data S4.

Taking into account the very slight La ion deficiencies for the compounds as measured by XRF, our calculations suggest that the  $n = 1$  and 2 phase were oxygen hyperstoichiometric with the  $\delta$  values of  $+0.18 \pm 0.03$  and  $+0.08 \pm 0.05$ , respectively. The  $\delta$  value obtained for the  $n = 2$  compound of  $+0.08$ , is similar to other reported values of  $-0.05$  [5],  $-0.08$  [6],  $-0.07$  [18] and  $+0.03$  [18]. The  $\delta$  value obtained for the  $n = 1$  compound is similar to other reports in the literature ( $\delta$ , range in literature = 0 to  $+0.26$ ) [4,5,47–49,53–57]. In contrast, the  $n = \infty$  compound was found to be slightly oxygen deficient with the  $\delta$  value of  $-0.09 \pm 0.02$ , which is also similar to reported literature values of  $-0.14$  to 0 [14,15,58–61]. Finally, for the  $n = 3$  compound, the calculated  $\delta$  value of

$-0.46 \pm 0.06$ , suggested it is highly oxygen deficient. This  $\delta$  value was relatively larger than those previously reported ( $\delta$ , range in literature of  $-0.25$  to  $+0.02$ ) [5,6,18] and was assumed due to the differing conditions of synthesis and particle properties (e.g. small particle size) of this material compared with those reported in the literature.

## 5. Conclusions

We successfully achieved our initial objectives to synthesize some target phases in the La–Ni–O series using a direct and efficient method. As expected, greater intimacy of the two component metal hydroxides (i.e. in the HFC route) led to a more facile synthesis compared with more conventional synthesis methods. Under the experimental conditions employed, our target materials were obtained via single heat treatments in a furnace from “co-crystallized” reagents prepared using the continuous hydrothermal flow synthesis (CHFS) system. Among the most noteworthy results herein,  $\text{La}_3\text{Ni}_2\text{O}_7$  and  $\text{La}_4\text{Ni}_3\text{O}_{10}$  were synthesized via single 12 h heat treatments in air at 1150 and 1075 °C, respectively, from the corresponding metal hydroxide co-crystallites. The synthesis of  $\text{La}_4\text{Ni}_3\text{O}_{10}$  phase was reduced even further down to 6 h at 1075 °C, from another co-crystallized powder, which was made under more severe conditions and in the presence of peroxide. These results are significant, as the higher order RP phases ( $n = 2$  and 3) are usually synthesized through several days of multiple regrinding and heating. In this regard, our development of a direct route to heterometallic oxides, some of which are conventionally laborious to make, may allow high throughput approaches to be developed for oxide materials discovery. We are currently investigating this very concept, the results of which will be reported in due course.

## Acknowledgment

EPSRC is thanked for funding the “High Throughput Inorganic Nanomaterials Discovery” project [EPSRC Grant Reference: EP/D038499/1] (JAD, SK) and an industrial case award (PB). The School of Engineering and Material Sciences at QMUL is thanked for a scholarship (XW). Johnson Matthey is thanked for supporting the industrial case award (PB). M. Phillips, V. Ford, J. Caulfield, M. Willis and Z. Luklinska are thanked for technical assistance.

## Appendix A. Supplementary data

Supplementary data associated with this article can be found in the online version at doi:10.1016/j.jssc.2008.02.006.

## References

- [1] P. Lacorre, J. Solid State Chem. 97 (1992) 495–500.
- [2] S.N. Ruddlesden, P. Popper, Acta Crystallogr. 11 (1958) 54.

- [3] J.D. Jorgensen, B. Dabrowski, S. Pei, D.R. Richards, D.G. Hinks, *Phys. Rev. B* 40 (1989) 2187–2199.
- [4] K. Ishikawa, W. Shibata, K. Watanabe, T. Isonaga, M. Hashimoto, Y. Suzuki, *J. Solid State Chem.* 131 (1997) 275–281.
- [5] G. Amow, I.J. Davidson, S.J. Skinner, *Solid State Ionics* 177 (2006) 1205–1210.
- [6] Z. Zhang, M. Greenblatt, J.B. Goodenough, *J. Solid State Chem.* 108 (1994) 402–409.
- [7] C.D. Ling, D.N. Argyriou, G. Wu, J.J. Neumeier, *J. Solid State Chem.* 152 (2000) 517–525.
- [8] Z. Zhang, M. Greenblatt, *J. Solid State Chem.* 117 (1995) 236–246.
- [9] M.D. Carvalho, M.M. Cruz, A. Wattiaux, J.M. Bassat, F.M.A. Costa, M. Godinho, *J. Appl. Phys.* 88 (2000) 544–549.
- [10] M.D. Carvalho, A. Wattiaux, J.M. Bassat, J.C. Grenier, M. Pouchard, M.I.D. Pereira, F.M.A. Costa, *J. Solid State Electrochem.* 7 (2003) 700–705.
- [11] K. Sreedhar, M. McElfresh, D. Perry, D. Kim, P. Metcalf, J.M. Honig, *J. Solid State Chem.* 110 (1994) 208–215.
- [12] K. Sreedhar, J.M. Honig, M. Darwin, M. McElfresh, P.M. Shand, J. Xu, B.C. Crooker, J. Spalek, *Phys. Rev. B* 46 (1992) 6382.
- [13] A. Martinez-Juarez, L. Sanchez, E. Chinarro, P. Recio, C. Pascual, J.R. Jurado, *Solid State Ionics* 135 (2000) 525–528.
- [14] A. Ghosh, A.K. Raychaudhuri, R. Sreekala, M. Rajeswari, T. Venkatesan, *J. Phys. D—Appl. Phys.* 30 (1997) L75–L79.
- [15] A. Tiwari, K.P. Rajeev, *J. Phys. Condens. Matter* 11 (1999) 3291–3298.
- [16] S.K. Tiwari, J.F. Koenig, G. Poillerat, P. Chartier, R.N. Singh, *J. Appl. Electrochem.* 28 (1998) 114–119.
- [17] G. Amow, S.J. Skinner, *J. Solid State Electrochem.* 10 (2006) 538–546.
- [18] M.D. Carvalho, F.M.A. Costa, I.D.S. Pereira, A. Wattiaux, J.M. Bassat, J.C. Grenier, M. Pouchard, *J. Mater. Chem.* 7 (1997) 2107–2111.
- [19] A.A. Galkin, B.G. Kostyuk, V.V. Lunin, M. Poliakoff, *Angew. Chem. Int. Ed.* 39 (2000) 2738–2740.
- [20] P. Boldrin, A.K. Hebb, A.A. Chaudhry, L. Otley, B. Thiebaut, P. Bishop, J.A. Darr, *Ind. Eng. Chem. Res.* 46 (2007) 4830–4838.
- [21] T. Adschiri, Y. Hakuta, K. Kanamura, K. Arai, *High Pressure Res.* 20 (2001) 373–384.
- [22] A. Cabanas, J.A. Darr, E. Lester, M. Poliakoff, *Chem. Commun.* (2000) 901–902.
- [23] A. Cabanas, J.A. Darr, E. Lester, M. Poliakoff, *J. Mater. Chem.* 11 (2001) 561–568.
- [24] L.J. Cote, A.S. Teja, A.P. Wilkinson, Z.J. Zhang, *Fluid Phase Equilib.* 210 (2003) 307–317.
- [25] K. Kanamura, T. Umegaki, K. Toyoshima, K.I. Okada, Y. Hakuta, T. Adschiri, K. Arai, *Electroceram. in Japan III* 181-1 (2000) 147–150.
- [26] K. Kanamura, A. Goto, R.Y. Ho, T. Umegaki, K. Toyoshima, K. Okada, Y. Hakuta, T. Adschiri, K. Arai, *Electrochem. Solid State Lett.* 3 (2000) 256–258.
- [27] J. Lee, A.S. Teja, *J. Supercrit. Fluid.* 35 (2005) 83–90.
- [28] J. Lee, A.S. Teja, *Mater. Lett.* 60 (2006) 2105–2109.
- [29] N. Millot, B. Xin, C. Pighini, D. Aymes, *J. Eur. Ceram. Soc.* 25 (2005) 2013–2016.
- [30] A.A. Chaudhry, S. Haque, S. Kellici, P. Boldrin, I. Rehman, A.K. Fazal, J.A. Darr, *Chem. Commun.* (2006) 2286–2288.
- [31] E. Lester, P. Blood, J. Denyer, D. Giddings, B. Azzopardi, M. Poliakoff, *J. Supercrit. Fluid.* 37 (2006) 209–214.
- [32] Y. Hakuta, H. Ura, H. Hayashi, K. Arai, *Mater. Lett.* 59 (2005) 1387–1390.
- [33] A.C. Larson, R.B. Von Dreele, Los Alamos National Laboratory Report LAUR 8 (1986) 748.
- [34] X. Weng, P. Boldrin, I. Abrahams, S.J. Skinner, J.A. Darr, *Chem. Mater.* 19 (2007) 4382–4384.
- [35] J.D.G. Fernandes, D.M.A. Melo, L.B. Zinner, C.M. Salustiano, Z.R. Silva, A.E. Martinelli, M. Cerqueira, C. Alves Jr., E. Longo, M.I.B. Bernardi, *Mater. Lett.* 53 (2002) 122–125.
- [36] A.K. Norman, M.A. Morris, *J. Mater. Process. Technol.* 92–93 (1999) 91–96.
- [37] C. Shivakumara, M.S. Hegde, A.S. Prakash, A.M.A. Khadar, G.N. Subbanna, N.P. Lalla, *Solid State Sci.* 5 (2003) 351–357.
- [38] Y.P. Wang, J.W. Zhu, X.J. Yang, L.D. Lu, X. Wang, *Mater. Res. Bull.* 41 (2006) 1565–1570.
- [39] G. Amow, J. Au, I. Davidson, *Solid State Ionics* 177 (2006) 1837–1841.
- [40] V.A. Tsipouriari, X.E. Verykios, *J. Catal.* 187 (1999) 85–94.
- [41] Z.L. Zhang, X.E. Verykios, *Catal. Lett.* 38 (1996) 175–179.
- [42] Z.L. Zhang, X.E. Verykios, *Appl. Catal. A* 138 (1996) 109–133.
- [43] A.N. Shirsat, M. Ali, K.N.G. Kaimal, S.R. Bharadwaj, D. Das, *Thermochim. Acta* 399 (2003) 167–170.
- [44] H.E. Hofer, W.F. Kock, *J. Electrochem. Soc.* 140 (1993) 2889–2894.
- [45] M. Zinkevich, F. Aldinger, *J. Alloys Compds.* 375 (2004) 147–161.
- [46] J.R. Jurado, *J. Mater. Sci.* 36 (2001) 1133–1139.
- [47] M.L. Fontaine, C. Laberty-Robert, A. Barnabe, F. Ansart, P. Tailhades, *Ceram. Int.* 30 (2004) 2087–2098.
- [48] M.L. Fontaine, C. Laberty-Robert, M. Verelst, J. Pielaszeck, P. Lenormand, F. Ansart, P. Tailhades, *Mater. Res. Bull.* 41 (2006) 1747–1753.
- [49] C. Li, T.H. Hu, H. Zhang, Y. Chen, J. Jin, N.R. Yang, *J. Membrane Sci.* 226 (2003) 1–7.
- [50] S.J. Skinner, J.A. Kilner, *Solid State Ionics* 135 (2000) 709–712.
- [51] H. Falcon, A.E. Goeta, G. Punte, R.E. Carbonio, *J. Solid State Chem.* 133 (1997) 379–385.
- [52] B. Grande, H. Mullerbuschbaum, *Z. Anorg. Allg. Chem.* 433 (1977) 152–156.
- [53] A. Demourgues, F. Weill, J.C. Grenier, A. Wattiaux, M. Pouchard, *Physica C* 192 (1992) 425–434.
- [54] A. Demourgues, P. Dordor, J.P. Doumerc, J.C. Grenier, E. Marquestaut, M. Pouchard, A. Villesuzanne, A. Wattiaux, *J. Solid State Chem.* 124 (1996) 199–204.
- [55] T. Kyomen, M. Oguni, M. Itoh, K. Kitayama, *Phys. Rev. B* 60 (1999) 815–821.
- [56] S.J. Skinner, *Solid State Sci.* 5 (2003) 419–426.
- [57] H. Tamura, A. Hayashi, Y. Ueda, *Physica C* 258 (1996) 61–71.
- [58] M.T. Colomer, D.A. Fumo, J.R. Jurado, A.M. Segadaes, *J. Mater. Chem.* 9 (1999) 2505–2510.
- [59] V.F. Savchenko, L.S. Ivashkevich, I.Y. Lyubkina, *Zh. Neorg. Khim.* 33 (1988) 30–33.
- [60] S.P. Skaribas, P.J. Pomonis, A.T. Sdoukos, *J. Mater. Chem.* 1 (1991) 781–784.
- [61] J. Takahashi, T. Toyoda, T. Ito, M. Takatsu, *J. Mater. Sci.* 25 (1990) 1557–1562.
- [62] M. Zinkevich, N. Solak, H. Nitsche, M. Ahrens, F. Aldinger, *J. Alloys Compds.* 438 (2007) 92–99.
- [63] D.O. Bannikov, V.A. Cherepanov, *J. Solid State Chem.* 179 (2006) 2721–2727.